Fabrication of a Flexible Si-cotton Filter Membrane for Efficient Hot Oil/Hot Water Separation

Fibers and Polymers 2022, Vol.23, No.3, 843-851
DOI 10.1007/s12221-022-3236-y

ISSN 1229-9197 (print version)
ISSN 1875-0052 (electronic version)

Fabrication of a Flexible Si-cotton Filter Membrane for Efficient Hot Oil/Hot Water Separation

Leila Ghorbani[1], Ali Khatibi[1,2], Saravana B. Basuvalingam[3], Daniela Caschera[4], and Babak Shokri[1,2]*

[1]*Laser and Plasma Research Institute, Shahid Beheshti University, Tehran 19839, Iran*
[2]*Faculty of Physics, Shahid Beheshti University, Tehran 19839, Iran*
[3]*Department of Applied Physics, Eindhoven University of Technology, 5600 MB, Eindhoven, The Netherlands*
[4]*Institute for the Study of Nanostructured Materials, 00015 Monterotondo (Rome), Italy*
(Received March 10, 2021; Revised June 8, 2021; Accepted June 20, 2021)

Abstract: Increasing oily industrial waste water at room and high temperatures has become one of the most significant threats to the global ecosystem. Finding a suitable method for separating hot-oil/water pollution with an appropriate filter is highly necessary to effectively solve this problem. In this study, high-temperature oil/water separation was achieved using a silicon-modified textile (Si-cotton) as a filter, which was fabricated using polydimethylsiloxane (PDMS) solution as the precursor and through plasma polymerization. The plasma polymerization generated a uniform micro and nanoscale hierarchical structure on the Si-cotton surface. Furthermore, XPS and FT-IR analysis showed the lowering of the O/C ratio on the Si-cotton surface with respect to the pristine textile, and the presence of silicon on the Si-cotton surface after the plasma process. The results of these factors can be critical in making the final hydrophobic/oleophilic behaviour of the textile. More importantly, the Si-cotton membrane was tested for the separation process of hot oil/hot water mixture, which showed an acceptable efficiency even after fifteen separation cycles. The findings offered a two-step method, efficient and green, which was capable of working well even at a high temperature, to fabricate a flexible and scalable Si-cotton textile filter for reducing the necessity of additional and complicated cooling processes in the presence of high-temperature oil/water mixture.

Keywords: Hot oil/Hot water separation, Coating, Plasma polymerization, Cotton textile, PDMS

Introduction

Increasing industrial activities may offer many benefits to countries. On the other hand, this progress increases industrial effluents and pollutions, especially oily waste water, which can affect the global ecosystem and cause substantial economic losses in the long run [1-8]. Many exciting and promising efforts have been done to solve this issue. For example, separating oil from water is one of the most profitable ways regarding non-secondary pollution [9-12]. Researchers have recently focused on developing unique filter fabrication with hydrophobic and oleophilic properties, which is considered a reliable solution for oil/water separation. Several studies have been conducted in the context of room temperature oil/water separation [13-16] by using different materials such as titanium dioxide (TiO_2) [17], polydimethylsiloxane (PDMS) [18], oxide nanoparticles like Fe_3O_4 [19], diamond-like carbon (DLC) [20], hexamethyldisiloxane (HMDSO) [21], silica nanoparticles [22], and bismuth oxybromide/ poly tetra-fluorinated wax (BiOBr/ PFW) [23]. Oxide nanoparticles are widely used to impart specific wettability behaviours to the surface. He *et al*. [24] fabricated a combination of TiO_2 nanoparticles through immersion and spraying techniques, which improved efficiency of the oil/water separation process. Ma *et al*. [25] proposed using electrospun polyimide nanofibers and polymerized polybenzoxazine to fabricate superhydrophobic/superoleophilic membrane. In another study, Liu *et al*. [13] fabricated a superhydrophobic/superoleophilic cotton with SiO_2 nanoparticles by using octadecyl trichlorosilane via the sol-gel method. Singh *et al*. [26] used zirconia particles for obtaining oil-water separation membranes. It should be noted that a combination of materials and techniques could be considered to fabricate an oil/water separation membrane. For example, in a study by Toro *et al*. [27], DLC film from plasma deposition and TiO_2 nanorods by sol-gel were used in synergy for obtaining a superhydrophobic/superoleophilic effect for a melamine sponge.

Despite the high efficiency of these methods, they usually require multiple chemical reactions and specific substrates such as meshes, which are not always scalable. More importantly, oil/water separation processes are normally conducted on room temperature and mixture. However, some industries such as refineries, petrochemical, textile, leather, and food factories, usually produce huge amounts of wastewater at temperatures varying from 25 °C to very high temperatures [28]. The previous materials/techniques have usually had good efficiency in separating oil/water mixture at room temperature. Nevertheless, scanty research has addressed the performance of hot mixture separation since high temperatures may impair the filter surface structures, which can negatively impact the oil/water separation ability [29]. One possible solution in the presence of a high-temperature mixture could be to lower the temperature of the mixture by an alternative cooling process. However, this solution could be very expensive in terms of spending much

*Corresponding author: b-shokri@sbu.ac.ir

time or using special systems for decreasing the temperature. Therefore, it is necessary to use new filters which can operate with good efficiency even at different and/or high temperatures. These kinds of filters could separate oil from water immediately after the output so as to decrease the operation time and the energy consumption. In this regard, it is interesting to develop materials and methods for filtering systems which can work in a wide range of temperatures with an eco-friendly, low consumption, low number of steps, and scalable manner.

This study presents the fabrication method of an efficient room temperature and hot oil/hot water separation membrane. A hydrophobic/oleophilic cotton textile is developed by plasma polymerization of PDMS solution, which is a green and economical source of Si-based polymers for plasma. Cotton is a low-cost material with excellent flexibility and can be considered as a suitable substrate to fit working conditions [30,31]. Furthermore, cotton surface with its hydrophilic hydroxyl groups can be easily functionalized by physical or chemical treatments and used for oil-water separation [32,33].

The wettability of a solid surface which repels or absorbs liquid is controlled by the chemical composition and the geometrical structure or morphology of the surface [34,35]. In this way, cold plasma technology has been chosen as a surface modification technique since it possesses the right promising potential to modify the wettability of cotton fiber surface without affecting the bulk properties of cotton and controlling the PDMS solution polymerization. Numerous active species in the plasma medium can incorporate new functional groups onto the surface of fibers [32,36-38], and the ion bombardment process in plasma can affect surface morphology [39]. Further, plasma polymerization is a gas-phase method, which is dry and eco-friendly (producing no liquid or toxic waste). In addition, even if a plasma apparatus is expensive, the aforementioned characteristics represent a great economical gain for industries, in comparison with the associated costs of other technologies, due to the transport, storage, safety of precursors/solvents, and environmental filters for liquid/gaseous wastes. Furthermore, plasma technologies can be scalable and easily introduced in producing an industrial process. Additionally, plasma polymerization, in comparison to other processes such as dip-coating and chemical methods, permits better control of the homogeneity and thickness of the coating deposited on the substrate. Furthermore, it adds the possibility to modify the surface appropriately, which can enhance adhesion and the durability of the coating [40,41]. These considerations, as well as the high versatility and reusability of the final proposed system, can positively affect the final cost of the product in the middle and long term.

HDMSO is usually used as Si precursors for plasma polymerization of Si-based films [21]. However, since it is highly flammable, it is not widely used in industry. In contrast, PDMS is another well-known Si-based polymer which could be considered a competitive alternative for Si precursor in plasma process deposition due to its no-toxicity and chemical inertness. Thanks to its high-performance properties like flexibility, thermo-tolerance, resistance to oxidation, tunable hardness, PDMS has been increasingly used in several fields, e.g., as an antifoaming agent in food application, an additive in cosmetics, and material for medical devices [42-44]. Furthermore, PDMS is extensively used to fabricate sponges for the oil/water separation process due to its intrinsic hydrophobicity [45]. To the best of our knowledge, scanty research has addressed the use of PDMS as Si precursors in plasma polymerization for modifying the wettability of the cotton surface. In this regard, the results indicated that plasma polymerization of PDMS solution on cotton permits creating micro and nano hierarchical structures and forming a Si-O-C polymeric film on the surface of cotton textiles. These changes are responsible for presenting hydrophobicity as well as oleophilicity of cotton textiles. The flexible Si-coated cotton membrane (Si-cotton) demonstrates up to 90 % efficiency in separating a 90 ^{o}C oil/water mixture without using any complicated method, a large amount of material, and a pre-cooling process. Additionally, the ability of the filter is not dramatically altered even after 15 separation cycles, which makes it an encouraging filter for practical applications even in hostile environments and the upcycling refining of the high temperature water.

Experimental

Materials

Cotton textiles were bought from a local store and cut into samples of equal size (10 cm×10 cm). Then, they were washed in a flask containing 5 wt% aqueous detergent solution. Cleaned samples were dried in an oven at 50 °C for 40 min. In order to prepare a suitable solution for the plasma polymerization process, PDMS (Dow Corning, Sylgard186 elastomer base-2 g) and PDMS precursor (Sylgard186 curing agent-0.2 g) were added to 50 m*l* of toluene to obtain a homogenous solution with low viscosity.

Plasma Polymerization

To fabricate the Si-cotton textile, PDMS-based plasma polymerization was conducted after Oxygen (O_2) plasma treatment. They were performed in a home-built low-pressure capacitively coupled plasma system driven by a power electrode with a diameter of 14 cm. The power electrode was connected to an automatic impedance matching network and operated at 13.56 MHz radiofrequency (RF). The cotton textile samples were placed on the power electrode in the plasma chamber.

O_2 plasma treatment was performed for 30 min on the cotton textiles at 25 °C, 20 W RF power, 20 sccm O_2 gas

flow, and 10 Pa working pressure. Plasma polymerization of PDMS-based solution was immediately performed on samples after O_2 plasma treatment. PDMS-based solution vapor was directly introduced into the plasma chamber by passing an argon gas flow as the carrier gas over the solution. Plasma polymerization was performed at 20 W RF power for 20 min and under 20 sccm of argon flow while the pressure of the plasma chamber was kept at 18.6 Pa.

Characterization

Chemical composition and bonding on the surface of cotton fibers were assessed by X-ray photoelectron spectroscopy (XPS) analysis using a Thermo Scientific KA1066 spectrometer with monochromatic Al Kα (with energy 1486.6 eV) X-ray radiation. Fourier transformed infrared (FTIR) spectra were recorded using the Thermo Nicolet model nexus 470 in the range of 500-4000 cm^{-1} to identify functional groups on the surface of the specimens. SEM images were collected using a Hitachi scanning electron microscope at an accelerating voltage of 15 kV. The samples were pre-coated with an ultra-thin layer of Au to prevent any changes.

Water Contact Angle (WCA) measurements were used to investigate the hydrophobicity of the samples. The analysis was performed using deionized water in the atmosphere at room temperature using the sessile drop method. A droplet of 4 μ*l* was dropped on the surface, and the reported contact angles were averaged over three measurements on different sample spots.

Laundry Test

This test was performed to evaluate the durability of the hydrophobicity of the surface. The Si-cotton samples (10 cm ×10 cm) were placed in a beaker with 200 m*l* distilled water at 80 °C and two magnets with about 2 cm inside. Then, they were left under magnetic stirring at an average speed of 600 rpm for 10 minutes. Next, the samples were dried in an oven at 50 °C. After each wash cycle, the contact angle was determined to assess the hydrophobicity degree. Five measurements were performed for each cycle and the averages were reported [46].

Separation Efficiency Measurements at Room and High Temperatures

To evaluate the Si-cotton textile separation efficiency, pump oil, gasoline, hexadecane, and paraffin were used to prepare room temperature mixture and hot oil/hot water mixture with the 1:1 volume ratio. This experimental condition was selected since it was very close to normally detectable and practical situations in which a hydrophobic/oleophilic filter, like Si-cotton system, is more suitable for oil/water separation, i.e. sampling of dispersion of oil in sea water or oil in the industrial wastewater stream.

For separating the hot mixture, the oil/water mixture was first prepared at room temperature in a beaker and then heated using a water bath at 100 °C due to the high flammability of some oils. The mixtures (at room temperature or at 90 °C as measured by thermometer) were poured on the Si-cotton and placed on a funnel. Next, efficiency was calculated by the following equation:

$$\text{Separation efficiency} = (V_1/V_0) \times 100$$

where V_1 is the volume of the water collected on the filter after the separation test, and V_0 denotes the starting volume of the initial water in the mixture before the separation test. The separation measurements were repeated 15 times for different oil/water mixtures. The results are reported in a graph for the first, fifth, tenth, and fifteenth cycles. The separation efficiency was calculated five times for each cycle, the average values were reported, and the errors were calculated as reported in [46].

Results and Discussion

XPS analysis was used to identify chemical compositions of Si-cotton textile (O2 plasma+plasma polymerization). The comparison of the full-range XPS spectra of pristine and Si-cotton samples (Figure 1(a)) shows a change in the relative intensity of C1s and O1s after plasma polymerization. The appearance of new Si peaks at binding energies of 101.9 and 152.8 eV, which were related to Si2p and Si2s on the Si-cotton surface (Figure 1(h)), indicates the success in using PDMS for modifying the surface of the cotton textile. In addition, atomic percentages of carbon, oxygen, and Si showed their incorporation to the cotton surface after the plasma process. Figures 1(b-d) and (f-h) show the detailed elemental composition of the Si-cotton membrane before and after PDMS-based polymerization.

C1s, O1s, and Si signals were examined to gain further insights into the chemical composition of the surface. As illustrated in Figure 1(b), the C1s spectrum of pristine cotton shows three peaks positioned at 284.78, 286.48, and 287.68 eV, related to C-C, C-O-C, and C=O bonds, respectively, which are common for a typical cotton textile [47]. It is evident that after plasma polymerization (Figure 1(f)), the relative intensity of C-C increases in comparison with pristine while C-O-C and C=O are reduced. In fact, PDMS-based plasma polymerization caused the incorporation of more carbon species, instead of oxygen, on the surface. On the other hand, the O1s spectrum (Figure 1(c)) demonstrates that three various components have been resolved. The binding energy around 532.58 eV was assigned to C-OH, which is related to unsaturated bonds on the surface. It was disappeared after plasma polymerization indicating that plasma polymerization makes unsaturated bonds on the surface passive (Figure 1(g)). The binding energies around 532.58 and 533.38 eV correspond to C-O and Si-O-C,

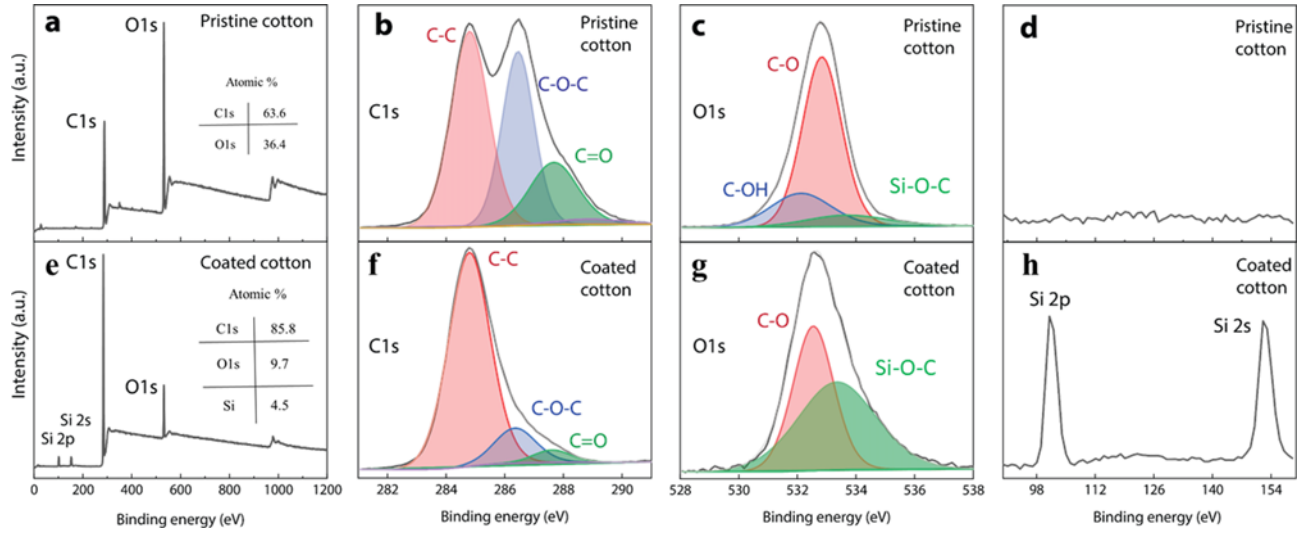

Figure 1. XPS survey spectrum of (a) pristine cotton textile, (b) C1s spectra of pristine cotton textile, (c) O1s spectra of pristine cotton textile, (d) Si spectra of pristine cotton textile, (e) Si-cotton (coated cotton) textile, (f) C1s spectra of Si-cotton textile, (g) O1s spectra of Si-cotton textile, and (h) Si spectra of Si-cotton textile.

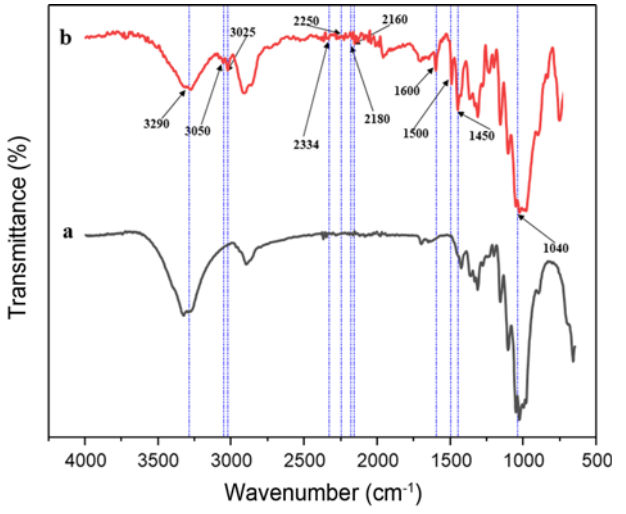

Figure 2. ATR-FTIR spectroscopy of (a) pristine cotton and (b) Si-cotton textile.

respectively [48].

Furthermore, based on the comparison of Figure 1(a) and Figure 1(e)-inset, the atomic C/O ratio increases from 1.75 to 8.85 after plasma polymerization. The relative percentage of Si on the Si-cotton increases by almost 4.5 %, which clearly indicates the success of polymerization and adding the Si-based coating to the cotton surface.

The ATR-FTIR measurement was performed to investigate the functional groups and Si-bonding on the Si-cotton surface. Figure 2 shows the ATR-FTIR spectra of pristine cotton and Si-cotton. Regarding pristine cotton (Figure 2(a)), the absorption peaks at 3335 and 2902 cm^{-1} correspond to O-H and asymmetric stretching vibration C-H, respectively. In addition, the peaks at 1054-1026 cm^{-1} are assigned to the C-O-C stretching vibration. This spectrum is similar to the typical FTIR spectra of cotton textile [39], which indicates the substrate is standard and has no additional material. After plasma polymerization of the PDMS-based solution, FTIR evaluation demonstrates multiple non-covalent interactions (Figure 2(b)). The bands at 1072 and 1007 cm^{-1} are considered as the main characteristic of Si-O-Si asymmetric and symmetric stretching vibrations. Asymmetric rocking at 864 cm^{-1} and stretching at 785 cm^{-1} vibrations can be attributed to the $Si-CH_3$ group [49,50]. The presence of methyl moieties in the modified surface is confirmed by an absorption band at 1410 cm^{-1}, which is related to CH_3 asymmetric bending in $Si-CH_3$ bonds, and by the bands at 2965 and 2906 cm^{-1}, which are the characteristic for asymmetric stretching and symmetric stretching of the CH_3 group, respectively [49,50]. The low-intensity band at 1450 cm^{-1} is assigned to the asymmetric bending vibrations of the CH_2 group in the $Si-CH_2-CH_2-Si$ link. The bands at 2100-2300 cm^{-1} correspond to Si-H stretching vibration while the stretching of C=O can be observed at 1629 cm^{-1} [49,50]. These peaks are absent in the FT-ATR spectrum of pristine cotton. Thus, these results indicate that cotton textile has been successfully modified by Si-based coating after plasma polymerization.

SEM images (Figure 3) show the morphology of cotton fibers before and after O_2 plasma and PDMS-based plasma polymerization. As shown in Figure 3(a), the surface of pristine cotton fibers is relatively smooth. In contrast, the surface morphology significantly alters after 30 min of O_2 plasma treatment, and many holes are created on the surface

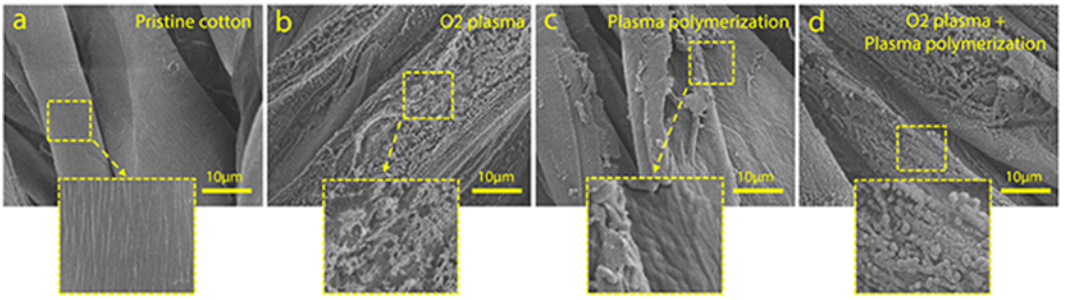

Figure 3. SEM images of (a) pristine cotton textile, (b) cotton textile after oxygen plasma pre-treatment, (c) cotton textile after plasma polymerization, and (d) cotton textile after plasma pre-treatment and plasma polymerization (Si-cotton).

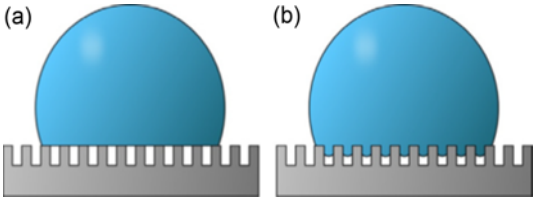

Figure 4. Cassie-Baxter and Wenzel wetting states on micrometer scale. (a) Cassie-Baxter wetting state and (b) hybrid wetting state where the liquid can partially penetrate air pockets in the surface [49].

due to plasma treatment (Figure 3(b)). Previous research has demonstrated that pre-treating the cotton surface with O_2 plasma treatment could dramatically impact surface properties by increasing the adhesion surface [51]. Figures 3(c-d) show the differences in final morphologies due to the previous O_2 plasma treatment. Figure 3(c) displays the irregular structures created on the surface fibers by plasma polymerization. Interestingly, after O_2 plasma treatment, plasma polymerization led to generating a lot of micro and nano hierarchical structures with a diameter of less than 1 μm (Figure 3(d)). Therefore, O_2 plasma treatment could efficiently increase the impact of plasma polymerization and create smaller and more homogenous structures on the surface.

The creation of micro and nanostructures on the surface increases hydrophobicity and oleophilicity. As shown in Figure 4, Cassie-Baxter's theory [52] explains that air pockets are formed in the gaps between these structures on the surface and micro/nanostructures, which result in water droplets on this structure [53].

In addition, creating these hierarchical structures affects the oleophilicity of the surface of the fiber due to the capillary effect [54]. Furthermore, the plasma polymerization in this study was performed using low power (20 W). In these conditions, few active radicals and ions were produced, and the rate of ionization was low. Therefore, the plasma process did not hurt the mechanical properties of the cotton bulk [55], which did not have any negative side in creating the hierarchical structure on the surface.

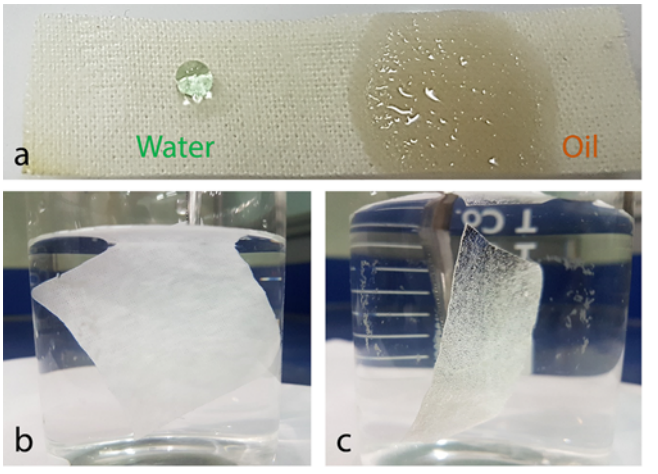

Figure 5. (a) Water and oil droplets on Si-cotton textil, (b) pristine cotton textile in water, and (c) Si-cotton textile in water.

Contact angle (CA) measurements were performed to evaluate the wetting properties of Si-cotton textiles. The presence of Si bonds with low surface energy on a surface is indicative of expecting a high water contact angle [56,57]. Additionally, increasing the intensity of C amount on the surface after PDMS-based polymerization, as previously observed by XPS, could be considered an essential parameter for increasing surface hydrophobicity [20].

As shown in Figure 5(a), the water and oil (gasoline) contact angles of the Si-cotton textile reach up to 144±3 and zero degrees, respectively. Such CA values confirm the hydrophobic/oleophilic behaviour of cotton after PDMS-based deposition, as it was predicted based on SEM and XPS results. It is worth noting that the water CA of pristine cotton textile is almost zero, and it absorbed water droplets.

Similar CA results by other systems such as DLC on cotton and dip-coating sponge in PDMS solution showed that the contact angle reached 143 ° and 150 °, respectively. In comparison to other works, the contact angles in this study indicated that the applied filter had a proper contact water angle due to its particular morphology [18,32].

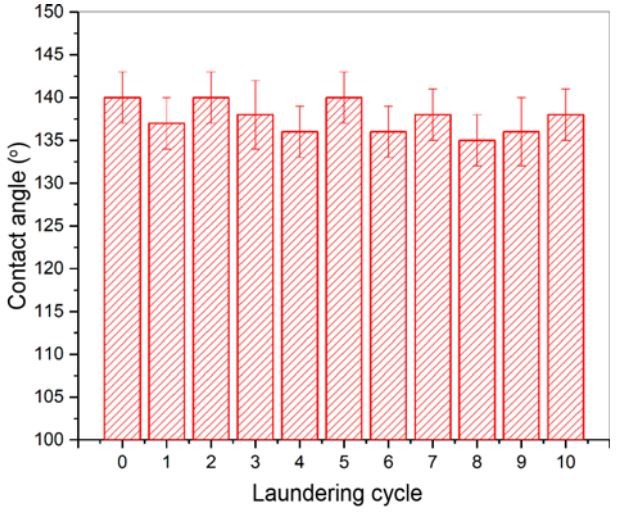

Figure 6. Variation of water contact angle of Si-cotton after laundering cycles at 80 °C.

Si-cotton and pristine cotton were immersed in water for a better comparison of the hydrophobicity behaviour. As observed in Figure 5(b), the pristine cotton is thoroughly wet while the Si-cotton textile (Figure 5(c)) floats on the water surface, and should be kept in the water. Furthermore, many air bubbles are formed on the textile surface. It is established that these air bubbles could be trapped between the micro- and nano-structures on the Si-cotton surface, which could significantly reduce the contact between water droplets and solid surface [53].

Laundering tests were performed to investigate the durability of Si-cotton. Figure 6 shows the contact angle of Si-cotton after each laundering cycle. It is noteworthy that the contact angle of Si-cotton varies after ten laundering cycles at 80 °C, which reaches the values in the range of 135 ° and 140 °. This behavior indicates that this system possesses high durability even after several laundry cycles at the high temperature condition (each cycle takes about 10 min; 10 cycles are equivalent to about 100 min washing).

The separation efficiency of the Si-cotton as a filter is evaluated at room temperature and 90 °C.

First, water is coloured (green) with food colouring to clarify the differences between water and transparent oils like pump oil. As shown in Figures 7(a-c), the prepared gasoline/water mixture is poured on the Si-cotton filter and fixed between the glass funnel and bottom tube (see movie S1). Oil passes quickly through the Si-cotton textile as a filter. Figure 7(c) demonstrates that no visible sign of gasoline could be detected in the (green) water at the top of the Si-cotton after separation.

The separation efficiency test was repeated in room temperature and hot mixtures of oils/water (paraffin, gasoline, pump oil, and hexadecane) (Figure 8). The pristine cotton obviously absorbs oil and water due to its intrinsic hydrophilic/oleophilic nature and cannot separate the mixture.

As depicted in Figure 8, the efficiency of Si-cotton textile is measured up to 15 separation cycles for room temperature mixture and hot mixture (90 °C). It is evident that the efficiency of mixture separation at 25 °C and 90 °C toward four different oils and the organic solvent is about 90 % even after 15 cycles. The morphology of the Si-cotton surface, similar to the blue lotus, and the variation of surface chemical composition, as mentioned in the XPS and SEM results, are considered as two essential factors for the

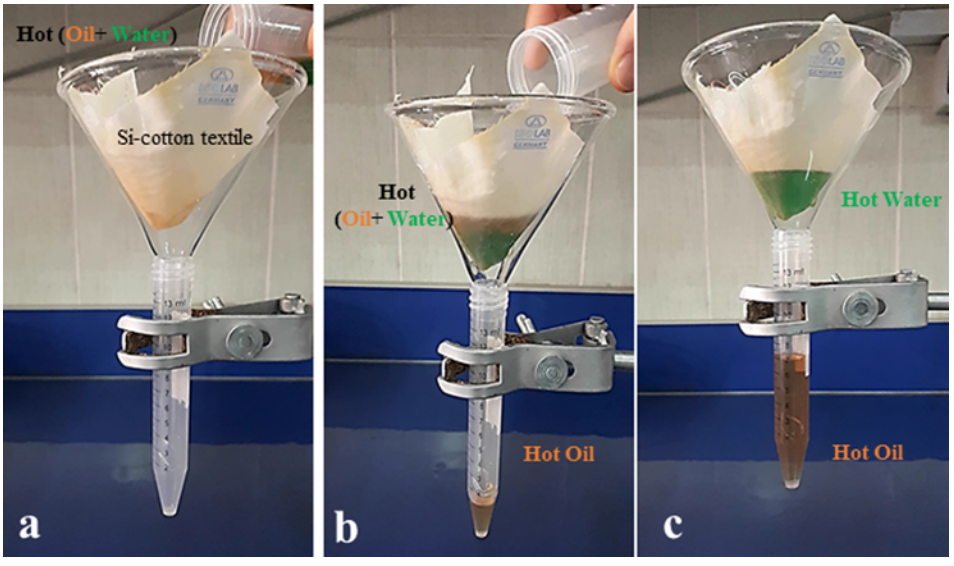

Figure 7. Sequence of photographs showing the process of separation of hot gasoline/hot water mixture; (a) The hot gasoline/hot water mixture is poured on the Si-cotton textile, (b) hot gasoline starts to pass the Si-cotton, and (c) hot water (in green) remains in the upper funnel while the hot gasoline is collected in the falcon tube.

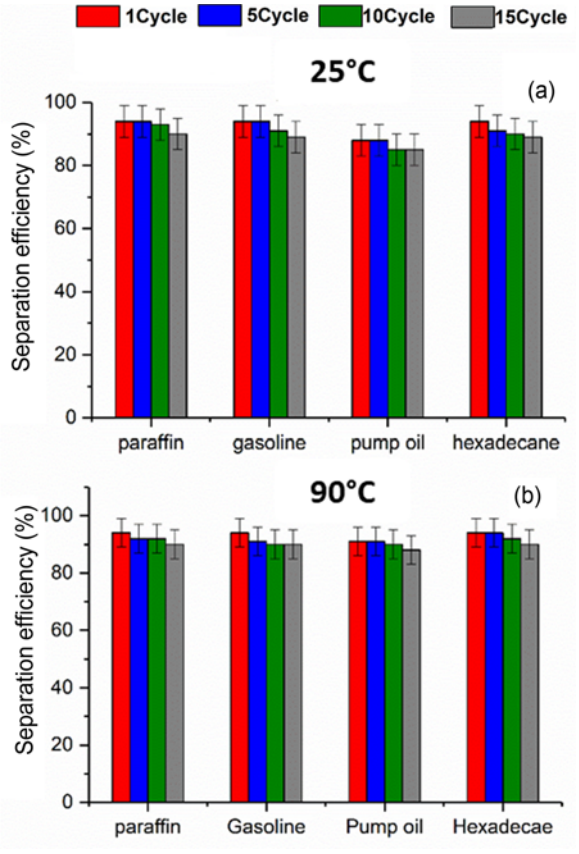

Figure 8. Separation efficiency of Si-cotton textile for various oil types and organic solvents/water mixture at (a) room temperature and (b) 90 °C, after different cycles.

behaviour of Si-cotton. In particular, regarding hot mixture separation experiments, the synergic effect of hierarchical structure and the presence of specific surface chemistry allow for obtaining an effective separation of the hot water from hot oil without any force. In general, 100 % efficiency indicates that the starting volume of water and sum of water after separation could be expected as equal at the end of the separation process. However, the results of this study showed that the volume of water before and after separation created a little difference because of two reasons. First, considering the natural porosity of the cotton substrate, it is reasonable to expect that a small amount of oil or water be trapped in the filter structure. However, the weight variation results of the filter were very small. In addition, the amount of oil or water retained to the filter fibers is considered as negligible, which may slightly affect the results in separation efficiency tests. Second, the slight decrease of efficiency could be ascribed to the effectiveness of the wettability property of the modified system. Even if the surface is hydrophobic, a little water with oil could sometimes pass through the cotton. In this study, all the water was retained with a little difference after separation. Although this difference is negligible, it might have a poor effect on the final efficiency. Hence, the amount of error by physical calculation was calculated and reported for the average separation efficiency with the error bar (Figure 8).

To prove the very good performances of the Si-cotton as an effective filter for separation even for the hot oil/water mixture, Table 1 shows a comparison of the oil/water separation efficiency between Si-cotton and other similar

Table 1. Comparison separation efficiency (SE) of different filters

Material	Method	Type of oils	SE of room temperature mixture	Number of cycle	SE of high temperature mixture	Number of cycle	Reference
PDMS	Plasma polymerization	Gasoline Hexadecane	90-95	15	90-95	15 (Hot oil/ Hot water)	This work
DLC	Coating by plasma	Pump oil	100	1	-		[20]
TiO_2	Hydrothermal	Petroleum	100	1	-		[58]
Acrylamide and acrylonitrile	Graft copolymerization	Crude Olive Diesel	95-99	1	-		[59]
SiO_2	Solution-blow spinning	Oil	20-10	1	-		[60]
HDTMS and SA	Dip coating	Hexadecane Diesel	100	1	-		[26]
GO@CNF	Electrospun	Hexane	100	10	-		[61]
Epoxy/attapulgite	Spray-coating	Paroline	98	10	-		[62]
PDA-Ca complex	Dip coating	Gasoline	-	-	97	80 (Hot water)	[5]
Polyurethane and silica nanoparticles	Spary	Kerosene	96	40	High	1 (Hot water)	[63]
PEDOT-PSS hydrogel	Chemical polymerization	Diesel	-	-	99	50 (Hot water)	[64]

filters. The performance of Si-cotton filter at room temperature is identical or even superior to other filters. It is evident that very few materials present acceptable efficiency for hot mixture separation, and even non-eco-friendly materials or complex methods and materials are usually used in that case. Furthermore, the reusability and separation efficiency of the high-temperature mixture have been rarely investigated thoroughly in upcycling. In contrast, the Si-cotton filter shows good performance in separating hot oil and hot water mixture, and it is fabricated using a greener method (i.e., PDMS-based plasma polymerization) as compared to other approaches such as electrospun or dip coating. These considerations make the Si-based cotton membrane a very appealing and suitable device for the hot oil/hot water separation process.

Conclusion

A two-step plasma treatment (O_2+PDMS-based plasma polymerization) was employed to fabricate a hydrophobic/oleophilic Si-cotton system. The high water contact angle and effective absorption of the oil on the Si-cotton surface confirmed the effectiveness of the fabrication method in controlling the surface wetting properties. In addition, due to the specific morphologies induced by plasma and the functionalities added to the substrate, the developed Si-cotton system was confirmed as an efficient filter for room temperature and hot oil/hot water separation, with an efficiency level which was higher than or comparable to other similar separation systems. In contrast to other filter materials, the fabrication of this system did not require multiple and/or environmentally toxic chemical reactions. The flexible nature, low production cost of the cotton substrate, and elimination of any other cooling processes before filtration of the hot oil/hot water mixture could be considered as some potential benefits for making this Si-cotton filter as a suitable candidate for the practical hot oils/water separation process even in challenging environmental conditions.

Acknowledgement

The authors are very thankful to Mr Saeed Javadi for his assistance in SEM imaging.

This work has been supported by the Plasma Laboratory in Shahid Beheshti University. The authors declare that this research has been carried out without receiving any specific grant from funding agencies in the public, commercial, or not-for-profit sectors.

Electronic Supplementary Material (ESM) The online version of this article (doi: 10.1007/s12221-022-3236-y) contains supplementary material, which is available to authorized users.

References

1. M. Padaki, R. S. Murali, M. S. Abdullah, N. Misdan, A. Moslehyani, M. A. Kassim, N. Hilal, and A. F. Ismail, *Desalination*, **357**, 197 (2015).
2. Q. Ma, H. Cheng, Y. Yu, Y. Huang, Q. Lu, S. Han, J. Chen, R. Wang, A. G. Fane, and H. Zhang, *Small*, **13**, 1700391 (2017).
3. L. N. Nthunya, L. Gutierrez, S. Derese, N. Edward, A. R. Verliefde, B. Mamba, and S. D. Mhlanga, *J. Chem. Technol. Biotechnol.,* **94**, 2757 (2019).
4. A. K. Singh and J. K. Singh, *Prog. Org. Coat.,* **131**, 301 (2019).
5. J. Wang, S. Liu, and S. Guo, *Appl. Surf. Sci*., **503**, 144180 (2020).
6. G. Mahmodi, S. Dangwal, P. Zarrintaj, M. Zhu, Y. Mao, D. N. Mcllroy, M. Saeb, V. Vatanpour, J. D. Ramsey, and S. Kim, *Sep. Purif. Technol.,* **240**, 116630 (2020).
7. W. Meng, P. Li, Y. Lan, X. Shi, S. Peng, H. Qu, and J. Xu, *Sep. Purif. Technol.,* **233**, 115988 (2020).
8. W. Ma, S. K. Samal, Z. Liu, R. Xiong, S. C. De Smedt, B. Bhushan, Q. Zhang, and C. Huang, *J. Memb. Sci.,* **537**, 128 (2017).
9. J. H. Lee, D. H. Kim, and Y. D. Kim, *J. Ind. Eng. Chem.*, **35**, 140 (2016).
10. J. Wang, F. Han, B. Liang, and G. Geng, *J. Ind. Eng. Chem.*, **54**, 174 (2017).
11. C. Yeom and Y. Kim, *J. Ind. Eng. Chem.*, **40**, 47 (2016).
12. X. Du, X. Huang, X. Li, X. Meng, L. Yao, J. He, H. Huang, and X. Zhang, *J. Colloid Interface Sci.,* **458**, 79 (2015).
13. F. Liu, M. Ma, D. Zang, Z. Gao, and C. Wang, *Carbohydr. Polym.*, **103**, 480 (2014).
14. J. Yuan, X. Liu, O. Akbulut, J. Hu, S. L. Suib, J. Kong, and F. Stellacci, *Nat. Nanotechnol.,* **3**, 332 (2008).
15. Y. Chu and Q. Pan, *ACS Appl. Mater. Interfaces*, **4**, 2420 (2012).
16. Q. Ma, H. Cheng, A. G. Fane, R. Wang, and H. Zhang, *Small*, **12**, 2186 (2016).
17. C. H. Xue, S. T. Jia, H. Z. Chen, and M. Wang, *Sci. Technol. Adv. Mater*., **9**, 035001 (2008).
18. Y. Jin, P. Jiang, Q. Ke, F. Cheng, Y. Zhu, and Y. Zhang, *J. Hazard. Mater.,* **300**, 175 (2015).
19. S. F. Chin, A. N. Binti Romainor, and S. C. Pang, *Mater. Lett.,* **115**, 241 (2014).
20. B. Cortese, D. Caschera, F. Federici, G. M. Ingo, and G. Gigli, *J. Mater. Chem. A.,* **2**, 6781 (2014).
21. S. Asadollahi, J. Profili, M. Farzaneh, and L. Stafford, *Materials*, **12**, 219 (2019).
22. D. Aslanidou, I. Karapanagiotis, and C. Panayiotou, *Prog. Org. Coat.,* **97**, 44 (2016).
23. B. Ge, X. Yang, H. Li, L. Zhao, G. Ren, X. Miao, X. Pu, and W. Li, *Colloids Surf. A Physicochem. Eng. Asp.,* **585**, 124027 (2020).

24. T. He, H. Zhao, Y. Liu, C. Zhao, L. Wang, H. Wang, Y. Zhao, and H. Wang, *Colloids Surf. A Physicochem. Eng. Asp.,* **585**, 124080 (2020).
25. W. Ma, M. Zhang, Z. Liu, M. Kang, and C. Huang, *J. Memb. Sci.,* **570-571**, 303 (2019).
26. A. K. Singh and J. K. Singh, *RSC Adv.,* **6**, 103632 (2016).
27. R. G. Toro, P. Calandra, F. Federici, T. de Caro, A. Mezzi, B. Cortese, A. L. Pellegrino, G. Malandrino, and D. Caschera, *J. Mater. Sci.,* **55**, 2846 (2020).
28. S. Rasouli, N. Rezaei, H. Hamedi, S. Zendehboudi, and X. Duan, *Mater. Des.*, **204**, 109599 (2021).
29. Y. Li, Z. Zhang, M. Wang, X. Men, and Q. Xue, *J. Mater. Chem. A*, **5**, 5077 (2017).
30. L. Xu, W. Wang, J. Deng, Y. Guo, R. Zhang, J. Yu, and F. Ji, *Text. Res. J.,* **89**, 2952 (2019).
31. G. Liu, W. Wang, and D. Yu, *Cellulose*, **26**, 3529 (2019).
32. D. Caschera, B. Cortese, A. Mezzi, M. Brucale, G. M. Ingo, G. Gigli, and G. Padeletti, *Langmuir*, **29**, 2775 (2013).
33. C. Jiang, W. Liu, Y. Sun, C. Liu M. Yang, and Z. Wang, *J. Appl. Polym. Sci*., **136**, 47005 (2019).
34. J. A. Juárez-Moreno, A. Ávila-Ortega, A. I. Oliva, F. Avilés, and J. V. Cauich-Rodríguez, *Appl. Surf. Sci.,* **349**, 763 (2015).
35. B. Cortese, D. Caschera, G. Padeletti, G. M. Ingo, and G. Gigli, *Surf. Innov.*, **1**, 140 (2013).
36. L. Xu, J. Deng, Y. Guo, W. Wang, R. Zhang, and J. Yu, *Text. Res. J*., **89**, 1853 (2019).
37. R. Molina, J. M. Teixidó, C. W. Kan, and P. Jovančić, *ACS Appl. Mater. Interfaces,* **9**, 5531 (2017).
38. L Ghorbani, A Khatibi, and B Shokri, *Iran. J. Phys. Res.,* **19**, 683 (2020).
39. D. Caschera, A. Mezzi, L. Cerri, T. de Caro, C. Riccucci, G. M. Ingo, G. Padeletti, M. Biasiucci, G. Gigli, and B. Cortese, *Cellulose*, **21**, 741 (2014).
40. J. Vasiljević, M. Gorjanc, B. Tomšič, B. Orel, I. Jerman, M. Mozetič, A. Vesel, and B. Simončič, *Cellulose*, **20**, 277 (2013).
41. K. Tsougeni, A. Tserepi, G. Boulousis, V. Constantoudis, and E. Gogolides, *Plasma Process. Polym.,* **4**, 398 (2007).
42. N. Atthi, W. Sripumkhai, P. Pattamang, O. Thongsook, A. Srihapat, R. Meananeatra, J. Supadech, N. Klunngien, and W. Jeamsaksiri, *Microelectron. Eng*., **224**, 111255 (2020).
43. U. Eduok, O. Faye, and J. Szpunar, *Prog. Org. Coat.,* **111**, 124 (2017).
44. T. Yabuta, E. P. Bescher, J. D. Mackenzie, K. Tsuru, S. Hayakawa, and A. Osaka, *J. Solgel Sci. Technol.*, **26**, 1219 (2003).
45. J.-H. Shin, J.-H. Heo, S. Jeon, J. H. Park, S. Kim, and H.-W. Kang, *J. Hazard. Mater.,* **365**, 494 (2019).
46. P. R. Bevington, D. K. Robinson, J. M. Blair, A. J. Mallinckrodt, and S. McKay, "Data Reduction and Error Analysis for the Physical Sciences", Vol. 7, p.415, Computers in Physics, University of California, USA, 1993.
47. M. Wang, X. Long, J. Du, C. Sun, S. Fu, and C. Xu, *Text. Res. J.,* **84**, 2149 (2014).
48. Y. Wang, M. Wang, J. Wang, H. Wang, X. Men, and Z. Zhang, *J. Taiwan Inst. Chem. Eng*., **99**, 215 (2019).
49. D. Cia, A. Neyer, R. Kuckuk, and H. M. Heise, *J. Mol. Struct*., **976**, 274 (2010).
50. D. Lin-Vien, N. B. Colthup, W. G. Fateley, and J. G. Grasselli, "The Handbook of Infrared and Raman Characteristic Frequency of Organic Molecules", p.251, Academic Press, California, USA, 1991.
51. Z. Wu, N. Xanthopoulos, F. Reymond, J. S. Rossier, and H. H. Girault, *Electrophoresis*, **23**, 782 (2002).
52. A. B. D. Cassie and S. Baxter, *Trans. Faraday Soc*., **40**, 546 (1994).
53. D. Caschera, R. G. Toro, F. Federici, C. Riccucci, G. M. Ingo, G. Gigli, and B. Cortese, *Cellulose*, **22**, 2797 (2015).
54. R. Jafari, S. Asadollahi, and M. Farzaneh, *Plasma Chem. Plasma Process.,* **33**, 177 (2013).
55. A. Zille, F. R. Oliveira, and A. P. Souto, *Plasma Process. Polym*., **12**, 98 (2015).
56. Y. Li, C. Zou, J. Shao, and Y. Li, *Text. Res. J.,* **89**, 401 (2019).
57. M. P. Gashti, F. Alimohammadi, and A. Shamei, *Surf. Coatings Technol.,* **206**, 3208 (2012).
58. S. Li, J. Huang, M. Ge, C. Cao, S. Deng, S. Zhang, G. Chen, K. Zhang, S. S. Al-Deyab, and Y. Lai, *Adv. Mater. Interfaces,* **2**, 1500220 (2015).
59. H. Hosseinzadeh and S. Mohammadi, *Water Air Soil Pollut.,* **225**, 2115 (2014).
60. B. Ye, C. Jia, Z. Li, L. Li, Q, Zhao, J. Wang, and H. Wu, *J. Appl. Polym. Sci*., **137**, 49103 (2020).
61. C. Ao, W. Yuan, J. Zhao, X. He, X. Zhang, Q. Li, T. Xia, W. Zhang, and C. Lu, *Carbohydr. Polym.,* **175**, 216 (2017).
62. J. Yang, Y. Tang, J. Xu, B. Chen, H. Tang, and C. Li, *Surf. Coat. Technol.,* **272**, 285 (2015).
63. M. Cao, X. Luo, H. Ren, and J. Feng, *J. Colloid Interface Sci.,* **512**, 567 (2018).
64. C. Teng, X. Lu, G. Ren, Y. Zhu, M. Wan, and L. Jiang, *Adv. Mater. Interfaces*, **1**, 1400099 (2014).